

Fast Purification of Recombinant Monomeric Amyloid- β from *E. coli* and Amyloid- β -mCherry Aggregates from Mammalian Cells

Amberley D. Stephens,* Meng Lu, Ana Fernandez-Villegas, and Gabriele S. Kaminski Schierle*

Cite This: *ACS Chem. Neurosci.* 2020, 11, 3204–3213

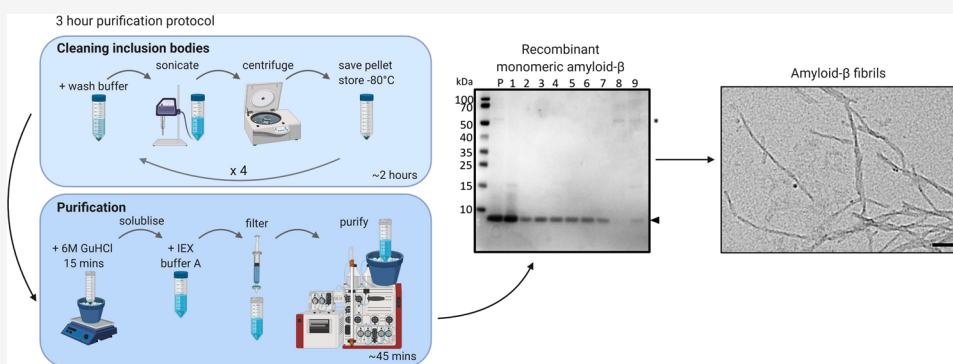
Read Online

ACCESS |

Metrics & More

Article Recommendations

Supporting Information



ABSTRACT: The Alzheimer's disease related peptide, Amyloid-beta ($A\beta$)1–40 and 1–42, has proven difficult to be purified as a recombinant monomeric protein due its expression in *E. coli* leading to the formation of insoluble inclusion bodies and its tendency to quickly form insoluble aggregates. A vast array of methods have been used so far, yet many have pitfalls, such as the use of tags for ease of $A\beta$ isolation, the formation of $A\beta$ multimers within the time frame of extraction, or the need to reconstitute $A\beta$ from a freeze–dried state. Here, we present a rapid protocol to produce highly pure and monomeric recombinant $A\beta$ using a one-step ion exchange purification method and to label the peptide using a maleimide dye. The washing, solubilization, and purification steps take only 3 h. We also present a protocol for the isolation of $A\beta$ -mCherry from mammalian cells.

KEYWORDS: $A\beta$ 42, $A\beta$ 40, E22G, arctic mutant, fluorescence, amyloid, ion exchange chromatography, maleimide, dye labeling, inclusion bodies, mCherry

INTRODUCTION

The presence of Amyloid-beta ($A\beta$) plaques and τ angles in neurons are hallmarks of Alzheimer's disease, therefore great research effort is put toward understanding how these initially soluble proteins misfold and contribute to pathology. To study protein misfolding, large quantities of protein are required, and while purification protocols for τ proteins are fairly well established, those for $A\beta$, in its isoforms of 1-39/43 and its mutant variants, are very heterogeneous and lead to variable products.¹

Many studies investigating aggregation rates and toxicity of $A\beta$ currently use synthetic $A\beta$ due to the ease of purchase and little handling required to obtain monomeric $A\beta$. However, $A\beta$ can be expensive to purchase and needs to be reconstituted to remove oligomers which can lead to loss of protein in the form of insoluble structures, protein adhering to centrifuge tubes, or buffer exchange steps. There is often variation in the resulting sample due to the use of different solvents for reconstitution, which can influence the initial structure.² Differences in disaggregation protocols can also introduce heterogeneous structures in the starting peptide, such as the use of hexafluoroisopropanol (HFIP) vs ammonium hydroxide.

HFIP is widely used to disaggregate $A\beta$, yet it can also lead to formation of oligomeric structures, as the peptide is brought to neutral pH via its isoelectric point.³ Ammonium hydroxide disaggregation has been shown to produce fewer oligomers and a more homogeneous solution compared to a HFIP prepared $A\beta$ solution. In comparison, the HFIP prepared $A\beta$ had increased aggregation propensity.⁴ Furthermore, synthetic $A\beta$ has been reported to have high batch variability and lower toxicity compared to recombinantly produced $A\beta$.^{5,6}

Purification of tagged- $A\beta$ is a highly popular method as addition of tags can improve solubility and permit the use of affinity capture chromatography, which can yield highly pure recombinant $A\beta$ samples. In a recent review on $A\beta$ purification methods, it was highlighted that 23/30 protocols utilized

Received: May 18, 2020

Accepted: September 22, 2020

Published: September 22, 2020



tagged- $A\beta$ for purification.¹ The added benefit of using a recombinant tagged system containing a cleavage site at the $A\beta$ N-terminus is that it can be utilized to release the wild-type $A\beta$ sequence without a methionine (M) start codon. *In vivo*, $A\beta$ is cleaved from the amyloid precursor protein; therefore, the first codon in the sequence is an aspartate, the sequence of which cannot be obtained by expressing $A\beta$ alone, and $A\beta$ M variants are instead used which have the methionine starting residue before aspartate. However, if tags are not removed prior to further analysis of the peptide, even a small tag, such as a 6xHis-tag, can greatly influence the protein structure and aggregation propensity.⁷ Moreover, removal of the tag requires the addition of a cleavage recognition site and additional purification steps which lead to loss of protein, increased time of protein handling, and therefore formation of aggregated species.

The protocol by Walsh *et al.* provided an easy method for purification of $A\beta$ M variants using urea solubilization to isolate $A\beta$ M from inclusion bodies, purification by ion exchange chromatography and size exclusion chromatography, centrifugation applying a 30 kDa filter, and lyophilization to store the recombinant protein.⁸ However, the DEAE-cellulose chromatography media used in the ion exchange step is no longer commercially available.

Reversed phase (RP) chromatography is another frequently used method to purify $A\beta$ due to the high purity of the resulting recombinant protein. $A\beta$ is eluted from the RP column along a gradient of organic solvent in the presence of an ioniser such as trifluoroacetic acid (TFA). The organic solvent is then removed by freeze-drying. The process of freeze-drying induces formation of oligomers, which subsequently can be removed by gel filtration, yet this adds another step to the purification protocol. We have shown for another amyloidogenic protein, α -synuclein, that freeze-drying leads to a compaction of the monomer structure and formation of heterogeneously sized oligomers, even after reconstitution in buffer, compared to samples that were frozen directly after purification.⁹ Freeze-drying could also affect the structure of monomeric $A\beta$, although further studies are needed to confirm this. As with all intrinsically disordered amyloidogenic proteins the structure of the starting material, e.g., the presence of multimers or degraded products, and the surrounding environment heavily influence the aggregation rate, the pathways of aggregation that are taken, and the toxicity of the resulting amyloid.²

Here, we provide an improved protocol circumventing some of the outlined issues raised above for the purification of recombinant $A\beta$ M42 and $A\beta$ MC40 from *E. coli*. The protocol utilizes a one-step ion exchange chromatography protocol from cleaned and solubilized inclusion bodies, removing the need for affinity tags, and the use of an ion exchange column is cheaper than a gel filtration column. The protocol is rapid, requiring just 45 min to solubilize and purify $A\beta$ M, reducing researchers' time and reducing the formation of oligomers. There is no requirement for a lyophilization step which can induce oligomer formation. The protocol can be amended to permit the incorporation of a maleimide dye label to the cysteine residue of mutated sequences, such as the $A\beta$ MC40 sequence. After induction of $A\beta$ M expression in *E. coli*, the purification protocol takes only around 3 h to obtain highly pure monomeric $A\beta$ M. We also present a protocol for the isolation of $A\beta$ M(E22G)-mCherry from HEK293 cells again using one-step ion exchange chromatography.

RESULTS

Thorough Washing of Inclusion Bodies Yields Pure Recombinant $A\beta$ M. $A\beta$ 42 and $A\beta$ 40 are the most abundant Alzheimer's disease-associated variants and will be used here to demonstrate the purification method.¹⁰ The $A\beta$ 40 variant used in this protocol contains an additional N-terminus cysteine residue, $A\beta$ MC40, which can be dye-labeled with thiol reactive dyes. $A\beta$ M42 and $A\beta$ MC40 were expressed from pET3a plasmids in *E. coli* BL21 (DE3) pLysS strain with 1 mM IPTG for 4 h. The *E. coli* cultures were centrifuged in 50 mL falcon tubes and the pellet stored at -80°C until needed (Figure 1, light blue box). During expression, $A\beta$ M peptides form into cytoplasmic insoluble inclusion bodies, which can be beneficial for the purification process as inclusion bodies can contain high quantities and purity of the protein of interest.¹¹ The inclusion bodies were thoroughly washed to obtain very pure inclusion bodies (Figure 1, medium blue box). The frozen

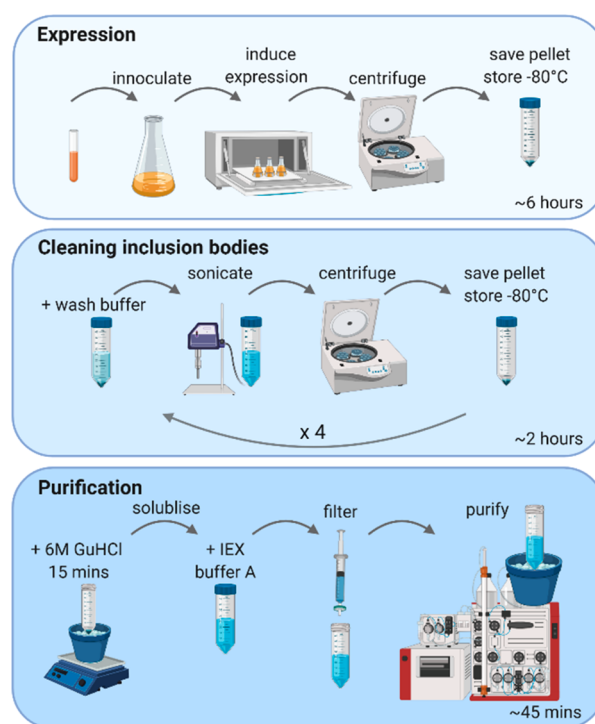


Figure 1. Schematic figure of the expression, isolation, and purification of $A\beta$ M42 and $A\beta$ MC40 from *E. coli*. Light blue box (top) – expression: An overnight culture was inoculated in lysogeny broth (LB) medium and then grown at 37°C until reaching an $\text{OD}_{600} \sim 0.6\text{--}0.8$. Expression of $A\beta$ M was induced upon addition of 1 mM IPTG, 4 h, after which the culture was centrifuged in 50 mL falcon tubes and the pellet stored at -80°C until use. Medium blue box (center) – cleaning inclusion bodies: $A\beta$ M is retained in insoluble inclusion bodies. The *E. coli* pellet was resuspended in wash buffer 1 (Table 1) and the inclusion bodies were isolated from the cells by sonication and centrifuged at 10,000g. The inclusion bodies were then washed three times with different buffers (Table 1) to remove unwanted proteins and lipids. The final inclusion body pellet was kept at -80°C until use. Dark blue box (bottom) – purification: The pellet of inclusion bodies was solubilized with $200\ \mu\text{L}$ of 6 M GuHCl per 50 mL of culture for 15 min on ice with a magnetic stirrer before dilution with 15 mL IEX buffer A. The protein solution was filtered through a $0.22\ \mu\text{m}$ membrane and purified using an ÄKTA FPLC with a HiTrap Q HP ion exchange column. Created with BioRender.com.

pellet from 50 mL of *E. coli* culture was resuspended in wash buffer 1 (Table 1) which contained protease inhibitors to

Table 1. Wash Buffer and Additives Used to Clean A β Containing Inclusion Bodies

10 mM Tris 1 mM EGTA pH 9			
Wash 1	Wash 2	Wash 3	Wash 4
protease inhibitors	protease inhibitors		
1 M GuHCl	1 M GuHCl		
1% Triton X-100	1% Triton X-100	1% Triton X-100	No additives

reduce proteolytic cleavage of A β M during cell lysis, 1 M guanidine hydrochloride (GuHCl) to increase washing efficiency by aiding the removal of other proteins, and 1% Triton X-100 to remove lipids bound to the inclusion bodies. The *E. coli* cells were sonicated 5 \times 30 s on ice and were centrifuged at 10,000g to remove cell debris. This was repeated three times with different additives in the wash buffer (Table 1). Although there was a loss of A β M during the wash steps, as observed in the supernatant of the washes in Supporting Information Figure 1, the cleaner the inclusion bodies then the higher the purity of the purified A β M. By the end of wash 4, the pellet contained highly pure inclusion bodies which were white in color, and which were subsequently stored at -80°C until solubilization and purification.

One-Step Ion Exchange Chromatography Yields Highly Pure Monomeric A β M. The A β M was solubilized from the inclusion bodies before purification. 200 μL of 6 M GuHCl was added to the inclusion body pellet from 50 mL of *E. coli* culture on ice. A small stir bar was added and the pellet left on a magnetic stirrer for 15 min to solubilize the inclusion bodies. GuHCl was chosen as a solubilizing agent instead of urea, as urea decomposition leads to isocyanic acid formation which can cause carbamylation of the N-terminus.¹² After 15 min, 15 mL of ice-cold ion exchange chromatography (IEX) buffer A (10 mM Tris, 1 mM EGTA pH 9) was added to the solution to dilute the GuHCl, reducing the ionic strength of the buffer to permit the protein to bind to the ion exchange column (Figure 1, dark blue box). The protein solution was

then filtered through a 0.22 μm filter to remove any precipitate before IEX. At this point, the A β M was already $\sim 90\%$ pure due to thorough washing of the inclusion bodies (Supporting Information Table 1). The fast protein liquid chromatography (FPLC) machine was not kept in a cold room; therefore, all buffers were kept on ice and an ice bag placed around the column to keep the system as cold as possible to reduce A β M aggregation. A HiTrap Q HP column (GE Healthcare) was used to purify the A β M monomer. To keep purification time to a minimum, the column was equilibrated in IEX buffer A prior to sample preparation. A β M was eluted over seven column volumes with a 0–100% gradient against IEX buffer B (10 mM Tris, 1 mM EGTA, 0.75 M NaCl, pH 9) followed by two column volumes at 100% buffer B. Absorption at 280 nm was used to monitor protein elution from the column (Figure 2a). Analysis of the eluted fractions by SDS-PAGE on a Coomassie blue stained gel showed pure monomeric A β M eluted at $\sim 30\%$ IEX buffer B (Figure 2, Supporting Information Figure 2). The concentration of A β M42 from each 1 mL fraction ranged 8–12.75 μM , determined by absorption at 280 nm and calculated using the extinction coefficient 1490 $\text{M}^{-1}\text{cm}^{-1}$ (Supporting Information Table 1). Purification of the A β MC40 variant is shown in Supporting Information Figure 3.

Recombinant A β M42 Forms Long Fibril-like Structures over Time. The recombinant A β M42 was analyzed by liquid chromatography mass spectrometry (LC-MS) to ensure a pure protein of the correct mass/charge had been purified. A deconvoluted mass of 4645 Da was obtained, which corresponded to the predicted mass of A β M42 (Figure 3a, m/z data presented in Supporting Information Figure 4.). To compare whether there were differences in the A β M42 product from different purification batches, such as the presence of degradation products or contaminants which may influence cell responses, we treated the neuronal cell line SHSY-5Y with A β M42 at 1–2 μM and investigated their vitality via metabolic activity using an MTT assay. We observed a slight, but not significant, increase in cell vitality upon the addition of A β M42 compared to cells without A β M42 treatment, which has previously been observed.¹³ No significant difference in cell vitality after treatment with A β M42 from batch 1 or 2 was

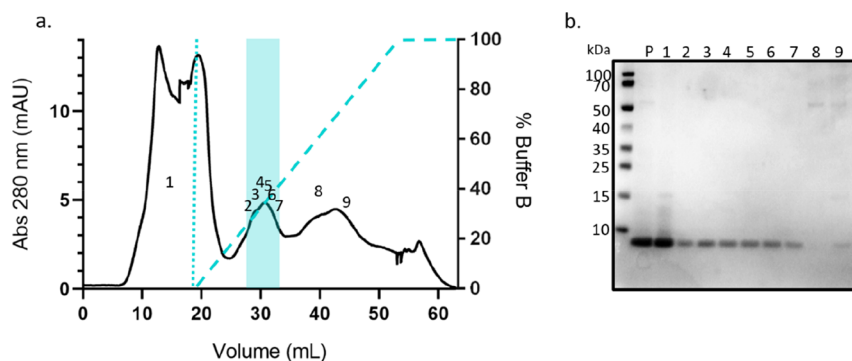


Figure 2. Highly pure monomeric A β M42 is purified by ion exchange chromatography from GuHCl solubilized inclusion bodies. A β M42 was solubilized in 6 M GuHCl and diluted in IEX buffer A before being applied to the HiTrap Q HP ion exchange column (shown up to the first dotted line in a). (a) Chromatograph of the absorption at 280 nm shows the elution of protein from the HiTrap Q HP column over a gradient of 0–100% buffer B containing 0.75 M NaCl over seven column volumes, followed by two column volumes of 100% buffer B (dashed line showing gradient in a). (b) In order to determine when A β M42 eluted from the column the fractions were collected and analyzed using SDS-PAGE on a 4–12% bis-tris gel with Coomassie blue staining. The numbers on chromatograph (a) correspond to the lane on the gel in (b). The A β M42 sample prior to IEX (P) was highly pure. Protein bands correlating to ~ 4.5 kDa (shown by the arrow next to b) show monomeric A β M42 in fractions 2–7 which are highlighted in blue in the chromatograph (a). A β M42 eluted at $\sim 30\%$ buffer B. Higher-molecular-weight species (indicated by a star in b) elute later in the buffer B gradient in fractions 8 and 9.

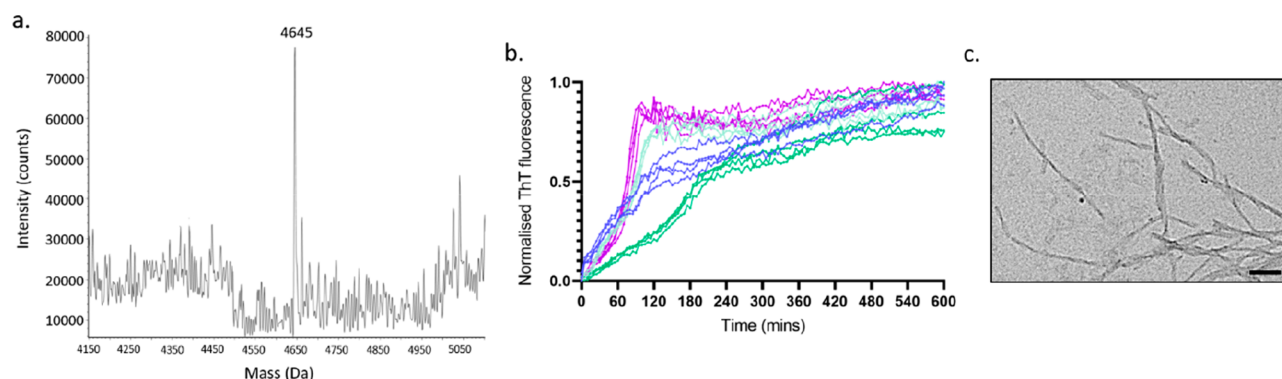


Figure 3. Pure recombinant $A\beta M42$ forms long fibrillar structures. Recombinant $A\beta M42$ was analyzed by mass spectrometry and the (a) deconvoluted spectrum shows the expected MW of 4645 Da (see Supporting Information Figure 4 for m/z spectrum). (b) Normalized ThT-based aggregation assays show slight batch variation (each color represents a batch), but good reproducibility within the batches (individual lines represent individual wells, four wells per batch). $5 \mu M$ of $A\beta M42$ in $100 \mu M$ Tris 200 mM NaCl, pH 7, with $20 \mu M$ of ThT was incubated in a half-area 96 well plate at 37°C with double orbital agitation at 300 rpm for 1 min before each read every 5 min for 600 min. (c) TEM image of fibrils formed during incubation of $5 \mu M$ of $A\beta M42$ with constant rotation at 20 rpm at 37°C for 2 days. Scale bar = 100 nm .

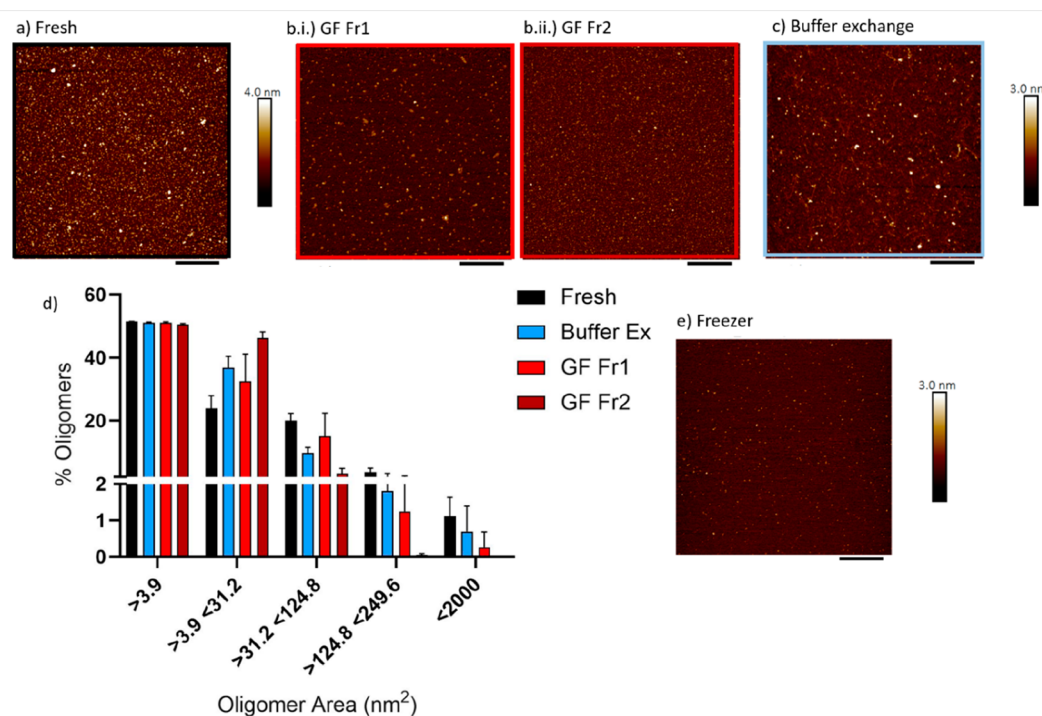


Figure 4. Atomic force microscopy shows that small multimeric $A\beta M42$ structures are present on mica, but most abundant after buffer exchange. $10 \mu L$ of $A\beta M42$ was deposited on freshly cleaved mica (a) directly after purification by IEX ($6.7 \mu M$), (b) after GF into 100 mM Na_2HPO_4 , pH 7, where $A\beta M42$ eluted between (i) 17.5 min ($8 \mu M$) and (ii) 18 min ($7 \mu M$), (c) after buffer exchange in cold 100 mM Na_2HPO_4 , pH 7, using PD MiniTrap G-10 columns ($5 \mu M$). (d) Size of the oligomers was extracted from each image and presented as a percentage of the total for each image and averaged for 6 images per condition. $3.9 \text{ nm}^2 = 1 \text{ pixel}$; $31.2 \text{ nm}^2 = 8 \text{ pixels}$; $124.8 \text{ nm}^2 = 32 \text{ pixels}$; $249.6 \text{ nm}^2 = 64 \text{ pixels}$. (e) $A\beta M42$ after storage at -80 for six months in IEX buffer A, pH 9, ($8 \mu M$) did not show large oligomeric structures. Black scale bar = 400 nm . The height profile bar shown at the right of the figure shows a height of up to 3–4 nm for multimeric species.

observed showing the purification protocol to reproduce recombinant $A\beta M42$ to a similar quality (Supporting Information Figure 5). A thioflavin-T (ThT) based aggregation assay was then used to investigate the aggregation properties of the purified $A\beta M42$ between batches. The ThT molecule fluoresces when it intercalates into the backbone of a fibril containing β -sheet structure, leading to a sigmoidal curve over time as the protein aggregates and the ThT fluorescence intensity increases.¹⁴ To investigate the aggregation propensity, $A\beta M42$ was diluted to $5 \mu M$ in 100 mM Tris, 200 mM NaCl,

pH 7, with $20 \mu M$ ThT and aggregated for 600 min with 1 min shaking at 300 rpm before every reading, every 5 min (Figure 3b). $A\beta M42$ aggregation was fairly rapid under the conditions used due to the presence of salt,¹⁵ although not all replicates show a clear lag phase, a sigmoidal curve of the increase of ThT fluorescence, as expected for a nucleation-dependent protein aggregation assay.¹⁶ Shown are $A\beta M42$ fibrils formed and imaged by transmission electron microscopy (TEM) (Figure 3c, Supporting Information Figure 6). Finally, we also show that during the solubilization step (Figure 1, medium

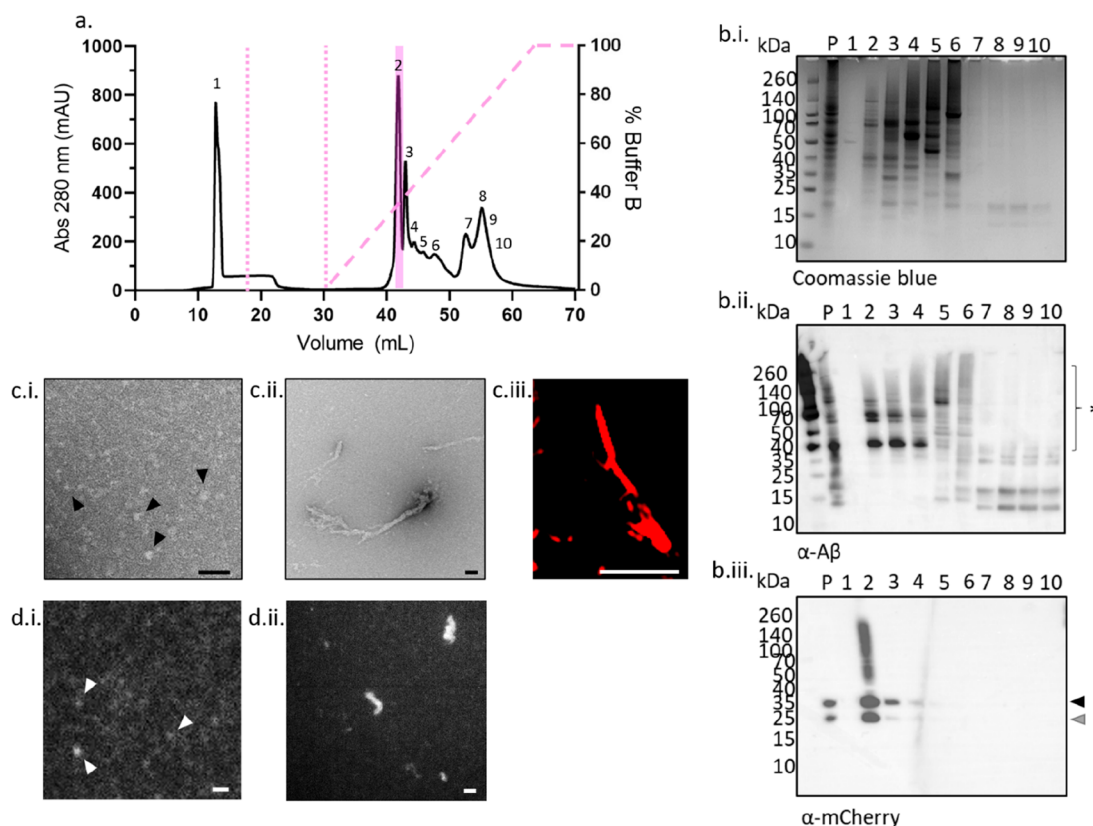


Figure 5. Varying aggregate sizes of $A\beta M(E22G)$ -mCherry isolated by ion exchange chromatography exhibit weak fluorescence. $A\beta M(E22G)$ -mCherry was lysed from HEK293 cells by sonication. (a) The soluble fraction was applied to the column (shown up to the first dotted line in (a)), and the unbound protein was washed from the column (shown up to the second dotted line in (a)). The chromatograph of absorption at 280 nm shows protein elution from the HiScreen Cpto Q ImpRes column eluted over a gradient of 0–100% of buffer B containing 1 M NaCl over seven column volumes, followed by two column volumes of 100% buffer B (dashed line showing gradient in (a)). (b) In order to determine when $A\beta M(E22G)$ -mCherry eluted off the column, the fractions were collected and analyzed using SDS-PAGE on a 4–12% bis-tris gel and (b.i) Coomassie blue staining, or transferred to a membrane for Western blot using antibodies against (b.ii) $A\beta$ and (b.iii) mCherry. The sample prior to IEX (P) contained many proteins, including aggregated $A\beta$ and mCherry. Protein bands correlating to ~ 32.3 kDa (shown by the black arrow in b.iii) show the predicted MW for monomeric $A\beta M(E22G)$ -mCherry. Fraction 2 contained the highest content of $A\beta M(E22G)$ -mCherry, although the presence of degraded mCherry (b.iii, gray arrow) and aggregated $A\beta$ (b.ii, star) was also apparent. The morphology of the purified $A\beta M(E22G)$ -mCherry was determined by TEM, and both (c.i) oligomers and (c.ii, Supporting Information Figure 8) larger aggregates were present. (c.iii) SIM image of a section view of an $A\beta M(E22G)$ -mCherry aggregate inside a cell prior to purification reveals a similar structure to those identified by TEM after purification. These purified aggregates were also analyzed to determine whether they were still fluorescent using wide-field imaging with a 561 nm laser, both (d.i) small oligomers and (d.ii) large aggregates were weakly fluorescent (also see Supporting Information Figure 9). Black scale bar = 100 nm; white scale bar = 2 μ m.

blue box), it is also possible to produce fluorescently labeled $A\beta$ via a dye-labeled cysteine modified $A\beta$, where the thiol-reactive dye reacts with the monomeric $A\beta$ as it becomes solubilized. 1 mM tris(2-carboxyethyl)phosphine (TCEP) was added to all buffers to keep the cysteine residue in a reduced form to allow the maleimide dye reaction to occur (Supporting Information Figure 7). The concentration of protein and degree of labeling (DOL) was calculated, taking into account the absorption of the dye at 490 nm and the influence of the dye on absorption at 280 nm (Supporting Information Table 2).

Buffer Exchange by Gel Filtration Is Preferable to Reduce $A\beta M42$ Oligomers Compared to Buffer Exchange Columns. $A\beta 42$ is the most aggregation-prone isoform of $A\beta$;¹⁷ it is therefore very difficult to maintain in a monomeric form during storage. Ideally, $A\beta M42$ would be purified and used straight away to prevent formation of multimeric or oligomeric structures; however, the purification buffer may not be ideal for many assays at pH 9. Two buffer exchange methods were compared to determine the extent of

oligomerization of the same aliquot of $A\beta M42$ when exchanged into 100 mM Na_2HPO_4 , pH 7, using PD MiniTrap G-10 buffer exchange columns (GE Healthcare) and a gel filtration column (GF) (Superdex 75 10/300 GL (GE Healthcare)) (Supporting Information Figure 8). Atomic force microscopy (AFM) was used to investigate presence of multimeric species (Figure 4 and Supporting Information Figure 9). The radius of gyration of $A\beta M42$ is ~ 0.9 nm¹⁸ and the resolution of the AFM images is 3.9 nm per pixel; therefore, multimers of $A\beta M42$ up to four are defined as one pixel, and surface-induced aggregation on the mica may increase the percentage of aggregates in comparison to that in solution.¹⁹ In comparison to freshly prepared $A\beta M42$ in pH 9 buffer and $A\beta M42$ buffer exchanged using G-10 buffer exchange columns with a gravity elution protocol, the $A\beta M42$ after GF had the least amount of oligomeric species, particularly the second fraction (dark red) collected which had a lower concentration (Figure 4a–d) (Figure 4c). Dependent on the downstream assays, the $A\beta M42$ is required for the G-10 columns provide a quick method for buffer exchange, but

A β M42 has begun to aggregate; yet, the use of a GF column takes longer, but yields a more monomeric protein. A β M42 which had been kept at $-80\text{ }^{\circ}\text{C}$ in pH 9 buffer had minimal aggregation (Figure 4e), yet prolonged storage at high pH may lead to chemical alteration of some residues.

A β M(E22G)-mCherry Purified from HEK293 Cells Remains Fluorescent. While purification of A β from *E. coli* is useful, as it produces a high quantity and purity, it is still unclear whether the monomeric and/or aggregate structures of A β formed *in vitro* are representative of those that form *in vivo*. Here, we present a protocol to isolate A β M(E22G)-mCherry from HEK293 cells. The A β E22G Alzheimer's disease associated mutant is highly aggregation prone.²⁰ Although the protein is tagged to a large fluorescent protein, mCherry, which may influence folding and structure, the fluorescent protein permits the study of A β aggregation in cells.²¹ In this cell line, we have previously identified five categories of intracellular A β M(E22G)-mCherry aggregates—oligomers, single fibrils, fibril bundles, clusters, and aggresomes. These stages underline the heterogeneity of A β 42 aggregates and represent the progression of A β 42 aggregation within the cell.²¹ Isolation of endogenous A β M(E22G)-mCherry may allow further insight into morphology or seeding ability of endogenously structured A β by microscopy.

Expression of A β M(E22G)-mCherry was induced by $1\text{ }\mu\text{g}/\text{mL}$ tetracycline for 7 days. The cells were centrifuged at 4000g for 15 min and the pellet was frozen until use. The cells were lysed by sonication in 50 mM Tris, pH 8, with protease inhibitors before centrifuging to separate the soluble and insoluble fractions. Western blot analysis, probing both A β and mCherry, showed that the soluble fraction contained more A β M(E22G)-mCherry than the insoluble fraction (Supporting Information Figure 10). The soluble fraction was purified using a HiScreen Capto Q ImpRes ion exchange column and eluted on a linear gradient against IEX buffer B (50 mM Tris, 1 M NaCl, pH 8) over seven column volumes, followed by two column volumes of 100% buffer B (Figure 5a). The eluted fractions were analyzed by SDS-PAGE separation and the gels were either stained with Coomassie blue (Figure 5b.i) or transferred onto a membrane and probed by Western blot for A β (Figure 5b.ii) and mCherry (Figure 5b.iii). The pre-IEX sample (P) contained many proteins (Figure 5b.i), yet a lot appeared to be aggregates of A β M(E22G) (Figure 5b.ii). Unbound proteins (Figure 5a, peak 1; b.i, lane 1) eluted from the column during the sample application and column wash. Peak 2, corresponding to lane 2 in Figure 5b contained the most abundant A β M(E22G) and mCherry by Western blot. The expected MW for monomeric A β M(E22G)-mCherry was 32.3 kDa (Figure 5b.iii, black arrow); therefore both degraded products (Figure 5b.iii, light gray arrow) and aggregated products were present (Figure 5b.ii, star). The presence of A β aggregates was to be expected as the E22G mutant is a highly aggregation prone mutant,²⁰ which was expressed in HEK cells for 7 days, and no denaturing step was employed during the purification protocol. It appears that mCherry is not always present in A β aggregates, as the Western blot displaying A β bound antibodies is more highly populated than the mCherry Western blot. It is possible that the A β M(E22G)-mCherry has become degraded in the cell; the expected molecular weight of mCherry is 26.7 kDa; therefore, mCherry fragments may be identified in the Western blot Figure 5b.iii. Another explanation for the discrepancy between the A β and mCherry probed blots may be due to steric hindrance preventing the

antibody binding to mCherry in an aggregated form. The concentration of fraction 2 was $77\text{ }\mu\text{M}$, as determined by absorption at 280 nm and calculated using the extinction coefficient of $35\,870\text{ M}^{-1}\text{ cm}^{-1}$.

The morphology and fluorescence of the purified A β M(E22G)-mCherry from peak 2 were analyzed by TEM and fluorescence microscopy. Both small oligomeric aggregates (Figure 5c.i, indicated by black arrows) and larger aggregates (Figure 5c.ii, Supporting Information Figure 11) were present. The large aggregates with fibrillar morphology were very similar to those identified within the cells using SIM imaging prior to purification (Figure 5c.iii).²¹ The aggregates also emitted weak fluorescence when excited with a 561 nm laser (Figure 5d.i, oligomers indicated with white arrows; and Figure 5d.ii, shows larger fluorescent aggregates, see also Supporting Information Figure 12). Mass spectrometry analysis of A β M(E22G)-mCherry showed the expected weight of the monomeric A β M(E22G)-mCherry, 32.3 kDa, was not highly abundant, but that a smaller degraded product of 25.2 kDa and a larger product of 36.3 kDa were the dominant species, among many other species of differing molecular weights (Supporting Information Figure 13). In cells, A β is commonly degraded or altered by post-translational modification; therefore, the presence of species of differing molecular weights of A β M(E22G)-mCherry may be reflective of different truncations and modifications that occur within a cellular environment.²²

CONCLUSION

We present a fast method for the purification of the Alzheimer's disease related peptide A β M. The benefits of this protocol include the use of commercially available reagents, a rapid one-step chromatography step using an ion exchange column and the lack of freeze-drying step which induces oligomerization and the need for further gel filtration steps requiring pricey columns. The purification protocol provided requires only 45 min to solubilize and purify, if the protein and buffers are kept ice-cold, highly pure monomeric recombinant A β M can be obtained. The protocol can be stopped and the products frozen at two key points, after centrifugation of *E. coli* expressing A β M, or after cleaning of the inclusion bodies prior to solubilization and purification. Ideally, A β M would be purified and used straight away to prevent freezing of monomeric peptide which can induce dimer and oligomer formation. Furthermore, we provide a protocol to isolate fluorescent A β M(E22G)-mCherry structures from mammalian cell lines which can be used to track seeding of A β in cells with fluorescent endogenously structured protein.

METHODS AND MATERIALS

Expression of Recombinant A β M Variants in *E. coli*. The plasmid pET3a containing human A β M42 and A β MC40 cDNA was transformed into *Escherichia coli* (*E. coli*) One Shot BL21 (DE3) pLysS (Thermo Fisher Scientific, USA). The plasmids were a kind gift from Prof. Sara Linse. The protein sequences encoded in the pET3a plasmids are A β M42: MDAEFRHDSGYEVHHQKLVFFAEDVGSNKGAIIGLMVGGVVIA and A β MC40: MCDAEFRHDSGYEVHHQKLVFFAEDVGSNKGAIIGLMVGGVV. One liter cultures of *E. coli* in Lysogeny Broth (LB) containing carbenicillin ($100\text{ }\mu\text{g}/\text{mL}$) were grown at $37\text{ }^{\circ}\text{C}$ with constant shaking at 250 rpm and induced for expression of A β M when the OD₆₀₀ reached 0.6–0.8 with addition of 1 mM isopropyl- β -thiogalactopyranoside (IPTG). After 4 h of A β M expression, the cells were pelleted by centrifugation in 50 mL falcon

tubes at $4000 \times g$ for 15 min. The supernatant is discarded, and at this point, the pellets can be frozen until further use.

Cleaning of A β M Containing Inclusion Bodies. 50 mL of culture from a 4 h induction (Table 1) was found to be a suitable amount for purification of monomeric A β M, as increasing the concentration can lead to aggregation during purification. At this point, multiple 50 mL pellets can be cleaned at the same time and frozen prior to solubilization and purification. The pellet was resuspended in 30 mL wash buffer 1 containing 10 mM Tris, 1 mM EDTA, protease inhibitor tablets (cOmplete EDTA-free cocktail, Roche), 1 M GuHCl, 1% Triton-X100, pH 9, and was sonicated on ice for 30 s on, 30 s off, five times using an XL-2020 sonicator (Heat Systems, USA). The suspension was centrifuged at 4 °C at $10,000 \times g$ for 15 min. The supernatant was discarded and the pellet was resuspended in 30 mL wash buffer 2 (Table 1) before sonicating it on ice for 30 s on, 30 s off, three times. The suspension was centrifuged at 4 °C at $10,000 \times g$ for 15 min. The supernatant was discarded and the pellet was resuspended in 30 mL wash buffer 3 (Table 1) before being sonicated on ice for 30 s on, 30 s off, three times. The suspension was centrifuged at 4 °C at $10,000 \times g$ for 15 min. The washing steps are important to remove impurities from the inclusion bodies and to obtain a high purity of the final recombinant A β M. At this point, the pellet should be white and can be frozen until use or solubilized before chromatography.

Solubilizing and Ion Exchange Chromatography of A β M.

The washed inclusion body pellet from 50 mL of culture was placed on ice with a small magnetic stir bar on a magnetic stirrer. 200 μ L of 6 M GuHCl was added to the pellet and stirred vigorously for 15 min to solubilize the A β M containing inclusion bodies. 15 mL of ice-cold IEX buffer A (10 mM Tris, 1 mM EDTA, pH 9) was added slowly to the solubilized pellet to dilute the 6 M GuHCl and to permit binding of A β M to the ion exchange column. The solubilized A β M was filtered through a 0.22 μ m filter before being placed on ice prior to chromatography. If the chromatography system is not kept in a cold room, then all buffers must be kept on ice and the column wrapped in an ice bag to keep the chromatography process as cold as possible to reduce aggregation of A β M. The ion exchange column must be equilibrated prior to the A β M sample being ready for purification to reduce the amount of time for A β M handling. A β M was loaded onto a HiTrap Q HP column (GE, Healthcare) and eluted against a linear gradient of IEX buffer B (10 mM Tris, 1 mM EDTA, 0.75 M NaCl, pH 9) over seven column volumes followed by two column volumes of 100% buffer B. Purification was performed on an ÄKTA Pure FPLC and monitored by absorption at 280 nm (GE Healthcare). A β M eluted at ~30% buffer B and must be immediately placed in aliquots for storage at -80 °C. The concentration of A β M was determined by absorption at 280 nm on a NanoVue spectrometer using the extinction coefficient of $1490 \text{ M}^{-1} \text{ cm}^{-1}$ for both A β M variants. A β M42 mass/charge was determined using ESI-MS at the Department of Chemistry, University of Cambridge. To note, for buffer exchange into required buffers for different assays, the fastest method is to use desalting columns and centrifugation. The PD MiniTrap G-10 columns (GE, Healthcare) are suitable for use with small peptides down to 700 Da.

Expression of Recombinant A β M(E22G)-mCherry in HEK293 Cells. The plasmid pcDNAS/FRT/TO:A β (E22G)-mCherry encodes the arctic mutant of A β 42 sequence (E22G) and a C-terminus encoded linker sequence GSAGSAAGSGESH followed by the mCherry fluorescent protein sequence. This plasmid was subsequently transfected along with the pOG44 plasmid encoding the FLP recombinase into the Flp-In T-REx-293 cell line (#R78007, Thermo Fisher Scientific). The gene of interest, the coding sequence of A β M(E22G)-mCherry, was integrated into the genome to generate an inducible, stable, and single-copy cell line expressing the Arctic mutant (E22G) of A β 42 fused to mCherry.²¹ Complete media (DMEM (high glucose), 10% FBS and 2 mM L-glutamine) was during cell line construction. Stable transfectants were selected using

complete media with the addition of the antibiotic hygromycin B for 6–12 weeks. After selection, single cell clones were collected to generate a homogeneous cell line and the expression level was characterized by flow cytometry in our previous paper.²¹

To induce A β M(E22G)-mCherry expression, we administered complete media with addition of 1 μ g/mL tetracycline to the cells. To harvest enough protein for purification, six T75 tissue flasks were seeded and cells induced for protein expression for 7 days. Approximately 12 million cells were collected and centrifuged at $4000 \times g$ for 15 min and directly frozen in -80 °C.

Purification of A β M(E22G)-mCherry. The HEK293 cell pellet was resuspended in 25 mL IEX buffer A (50 mM Tris, pH 8) with protease inhibitors (cOmplete, EDTA-free cocktail, Roche) and sonicated 20 s on, 30 s off, four times using an XL-2020 sonicator (Heat Systems). The suspension was centrifuged at $800 \times g$ for 5 min at 4 °C to remove unbroken cells. The supernatant was removed and centrifuged for a further 15 min at $21,000 \times g$ at 4 °C. The supernatant was saved as the soluble fraction, and the insoluble fraction was resuspended in IEX buffer A. To determine which fraction contained the most A β M(E22G)-mCherry the fractions were analyzed by SDS-PAGE on a 4–12% bis-tris gel and subjected to Western blot analysis to probe for the presence of A β and mCherry. The membrane was probed with an anti-A β antibody targeted to residues 1–16 (1:1000, #E 610, Biogen) and a secondary anti-mouse IgG HRP-conjugated antibody (1:1000, #NA931, GE Healthcare). The membrane was dried and reprobed with an anti-mCherry antibody (1:1000, #125096, abcam) and a secondary anti-mouse IgG HRP-conjugated antibody (1:1000, #NA931, GE Healthcare). The soluble fraction was found to contain more A β M(E22G)-mCherry than the insoluble fraction (Supporting Information Figure 10) and was therefore used for further purification. The soluble fraction was filtered through a 0.22 μ m membrane before being loaded on a HiScreen Canto Q ImpRes ion exchange column (GE Healthcare). The A β M(E22G)-mCherry was eluted from the column over seven column volumes on a linear gradient against IEX buffer B (50 mM Tris, 1 M NaCl, pH 8) followed by two column volumes of 100% buffer B. Western blot analysis, using the same antibodies as described above, was used to confirm in which eluted fractions the A β M(E22G)-mCherry resided. Monomeric A β M(E22G)-mCherry has a MW of 32.3 kDa, the Western blots show the presence of both degraded and aggregated A β M(E22G)-mCherry from purification. The A β M(E22G)-mCherry positive fraction was slightly pink in the column, but it is noted that the HEK293 cell medium is also pink and residues of the latter can be present in other eluted fractions; therefore, Western blot analysis is required to confirm the presence of A β M(E22G)-mCherry rather than just relying on color of eluted fractions. The concentration of the eluted fraction containing A β M(E22G)-mCherry was calculated from absorption at 280 nm on a NanoVue spectrometer using the extinction coefficient of $35,870 \text{ M}^{-1} \text{ cm}^{-1}$. A β M(E22G)-mCherry mass/charge was determined using ESI-MS at the Department of Chemistry, University of Cambridge.

SDS-PAGE and Western Blot. To determine in which fractions A β M eluted from the ion exchange columns, SDS-PAGE was run. 20 μ L of protein solution was incubated with 4 μ L of LDS sample buffer and incubated at 100 °C for 5 min before 10 μ L was loaded on a 4–12% bis-tris gel (NuPAGE, Thermo Fisher Scientific). The gel was either stained with Coomassie blue or transferred to a 0.22 μ m polyvinylidene fluoride (PVDF) membrane and probed for A β . The membrane was first blocked with 5% BSA in PBS with 0.05% Tween-20 for 30 min before incubation with the primary antibody against residues 1–16 of A β (1:1000, #E610, Biogen) for 1 h. After washing for 2 min three times, the membrane was incubated with the secondary antibody, anti-mouse IgG linked to HRP (1:1000, #NA931, GE Healthcare) for 1 h. The membrane was washed for 2 min five times and incubated with chemiluminescent substrate (SuperSignal WEST pico PLUS, Thermo Fisher Scientific) and imaged using a G:Box (Syngene). The membrane was dried and subsequently reprobed using similar conditions, by blocking with 5% BSA, incubating with the primary antibody against mCherry (1:1000,

#[1C51] ab125096, abcam) followed by washing and incubation with the secondary antibody anti-mouse IgG linked to HRP (1:1000, #NA931, GE Healthcare). To determine purity of the $A\beta$ M fractions, during purification the gel images were analyzed using ImageJ software²³ to determine the percentage of $A\beta$ M present. Regions of interest were selected with a rectangle and a histogram of the intensity of dyed protein within the area displayed using the measure function. From the peaks displayed in the histogram, correlating to protein bands, the percentage purity of $A\beta$ M could be calculated from the peak of $A\beta$ M as a percentage of the total area of peaks.

Cell Vitality Assays. Human neuroblastoma cells (SH-SY5Y) were obtained from the European Collection of Cell Cultures (ECACC, Sigma-Aldrich, Dorset, United Kingdom) and grown in a 1:1 minimal essential medium (MEM) (Sigma-Aldrich) and nutrient mixture Ham's F-12 (Sigma-Aldrich) supplemented with 15% FBS, 1% nonessential amino acids, 2 mM GlutaMAX, and 1% antibiotic–anti-mycotic (all Thermo Fisher Scientific, Epsom, United Kingdom). The vitality of neuroblastoma SH-SY5Y cells in the presence of $A\beta$ M42 was determined using the MTT (3 [4,5-dimethylthiazole 2]-2,5-diphenyltetrazolium bromide) kit from Promega (Madison, Wisconsin, US). Briefly, 3×10^4 cells were seeded into each well of 96-well culture plates overnight followed by incubation of $A\beta$ M42 from two purification batches at a final concentration of 1 and 2 μ M for 24 h. MTT was added to the cells for 4 h and the absorption was measured with a microplate reader at 590 nm (Envision, PerkinElmer, Waltham, Massachusetts, US). The absorbance is proportional to the number of viable cells. Each experiment was performed three times in duplicate for each purification batch. Data was normalized to the cell only control in each experiment.

Thioflavin-T (ThT) Based Kinetic Aggregation Assays. 20 μ M freshly made ThT (Abcam, Cambridge, UK) was added to 50 μ L of 5 μ M $A\beta$ M42 after buffer exchange into 100 mM Tris, 100 mM NaCl pH 7 using PD MiniTrap G-10 columns (GE, Healthcare). All samples were loaded onto nonbinding, clear-bottom, 96-well half area plates (Greiner Bio-One GmbH, Germany). The plates were sealed with a SILVERseal aluminum microplate sealer (Grenier Bio-One GmbH). Fluorescence measurements were taken with a FLUOstar Omega plate reader (BMG LABTECH GmbH, Ortenberg, Germany). The plates were incubated at 37 °C with double orbital shaking at 300 rpm for 1 min before each was read every 5 min for 600 min. Excitation was set at 440 nm with 20 flashes and the ThT fluorescence intensity measured at 480 nm emission with a 1300 gain setting. Two ThT assays were run using four fractions of $A\beta$ M42 from two purification runs with four wells per fraction. Data were normalized to the sample with the maximum fluorescence intensity for each plate.

Buffer Exchange. 300 μ L of $A\beta$ M42 at 25.5 μ M was buffer exchanged into 100 mM Na_2HPO_4 pH 7 using PD MiniTrap G-10 columns (GE Healthcare) following the gravity exchange protocol provided. The buffers were kept ice-cold to reduce oligomerization. 500 μ L of the same aliquot of $A\beta$ M42 at 25.5 μ M was also injected into a Superdex 75 10/300 GL gel filtration column. The 100 mM Na_2HPO_4 pH 7 buffer was kept on ice and the column wrapped in an ice bag to keep the protein as cold as possible. The $A\beta$ M42 was eluted isocratically at 0.8 mL/min and eluted between 17.5 and 18 min, as expected for a protein of 4.5 kDa.

Atomic Force Microscopy. 10 μ L of $A\beta$ M42 were incubated on freshly cleaved mica for 10 min while at 4 °C. The mica was washed five times with dH_2O and dried gently under a flow of compressed air. Images were acquired in Peak Force Quantitative Nanomechanical Property mode using ScanAsyst Air probes on a BioScope Resolve (Bruker AXS GmbH). Each field of view was 2 μ m \times 2 μ m acquired with 512 lines at 0.966 Hz. Images were flattened using NanoScope Analysis software, ver. 1.8 and exported. The pixel area of the oligomers was extracted from the AFM images using the ICY imaging software (<http://icy.bioimageanalysis.org/>) and were gray rendered before analysis. The area of oligomers was then calculated using the “Connected Components” plugin. The gray-scale 8-bit images were given a threshold of 80/256 to remove background and a group of

connected pixels was detected as a cluster which was converted to a size where one pixel = 3.9 nm².

Transmission Electron Microscopy of $A\beta$ M42 and $A\beta$ M(E22G)-mCherry Aggregates. 5 μ M of $A\beta$ M42 was incubated in 100 mM Tris 200 μ M NaCl, pH 7 for 2 days with constant rotation at 20 rpm on a rotator (SB2, Stuart Scientific) at 37 °C. $A\beta$ M(E22G)-mCherry was used at a concentration of 77 μ M. 10 μ L of each sample was deposited on a carbon 400 mesh grid for 1 min. The grid was washed twice for 15 s in dH_2O before incubating in 2% uranyl acetate for 30 s to negatively stain the sample. The grid was imaged using a Tecnai G2 80–200kv TEM at the Cambridge Advanced Imaging Centre.

Fluorescence Imaging of $A\beta$ MC40-AF488 and $A\beta$ M(E22G)-mCherry. A glass coverslip was cleaned with 1 M KOH for 15 min and washed extensively with dH_2O and dried. 5 μ M of $A\beta$ MC40-AF488 sample was incubated at 37 °C for 2 days with rotation at 20 rpm. The solution was centrifuged at 21,000 \times g for 5 min and 10 μ L deposited on the glass and incubated in the dark for 15 min. 10 μ L of $A\beta$ M(E22G)-mCherry at 77 μ M was deposited on the glass and incubated in the dark for 15 min. Both samples were washed three times to remove unbound protein with dH_2O and imaged. Images of the samples were collected using a custom-built three-color structured illumination microscopy (SIM) setup which we have previously described.²⁴ A 60 \times /1.2NA water immersion lens (UPLSAPO 60XW, Olympus) and a sCMOS camera (C11440, Hamamatsu) were used. The laser excitation wavelengths used were 488 nm (iBEM-SMART-488, Toptica) for imaging $A\beta$ MC40-AF488 and a 561 nm laser for $A\beta$ M(E22G)-mCherry (OBIS 561, Coherent). The samples were also imaged in the other laser channel and in the 640 nm laser (MLD 640, Cobolt) channel to check for cross talk or nonspecific fluorescence contaminants, no/little fluorescence was observed in other channels. The laser intensity used was between 10 and 20 W/cm² with an exposure time of 150 ms. Although a SIM setup was used, the intensity of the signal was too low in the samples to use artifact-free SIM reconstruction, so widefield reconstruction was used and the average intensity from nine SIM images is presented. The same setup was used to image $A\beta$ M(E22G)-mCherry aggregates in cells, but the signal was strong enough for SIM reconstruction, which was performed with LAG SIM, a custom plugin for Fiji/ImageJ available in the Fiji Updater. LAG SIM provides an interface to the Java 691 functions provided by fairSIM.²⁵

■ ASSOCIATED CONTENT

📄 Supporting Information

The Supporting Information is available free of charge at <https://pubs.acs.org/doi/10.1021/acschemneuro.0c00300>.

Coomassie stained gel of $A\beta$ M42 expression and cleaning of inclusion bodies in preparation for purification by chromatography; Ion exchange chromatography; Purity determined by densitometry and concentrations of fractions; Liquid chromatography and mass/charge spectrum; Viability of SHSY 5Y cells; Fibrillar structures formed after incubation of $A\beta$ M42; Formation of fluorescent fibrils and oligomers and purification by ion exchange chromatography; Calculation of the concentration and degree of labeling for eluted fractions containing $A\beta$ MC40-AF488; Atomic Force Microscopy; TEM showing purified fractions; Mass spectra; Raw images of Coomassie blue stained SDS PAGE gels and Western blots (PDF)

■ AUTHOR INFORMATION

Corresponding Authors

Amberley D. Stephens – Chemical Engineering and Biotechnology, University of Cambridge, Cambridge CB3 0AS,

United Kingdom; orcid.org/0000-0002-7303-6392;
Email: asds2@cam.ac.uk

Gabriele S. Kaminski Schierle – Chemical Engineering and Biotechnology, University of Cambridge, Cambridge CB3 0AS, United Kingdom; orcid.org/0000-0002-1843-2202;
Email: gsk20@cam.ac.uk

Authors

Meng Lu – Chemical Engineering and Biotechnology, University of Cambridge, Cambridge CB3 0AS, United Kingdom

Ana Fernandez-Villegas – Chemical Engineering and Biotechnology, University of Cambridge, Cambridge CB3 0AS, United Kingdom

Complete contact information is available at:

<https://pubs.acs.org/10.1021/acscemneuro.0c00300>

Author Contributions

A.D.S. designed experiments and performed purification, kinetic assays, AFM, TEM, and widefield microscopy imaging. M.L. constructed the A β M(E22G)-mCherry Flp-In T-REx-293 cell line and performed cell culture, performed SIM imaging, reconstruction of images of A β M(E22G)-mCherry in cells and helped with widefield microscopy imaging. A.F.-V. maintained SHSY-5Y cells and performed MTT assays. A.D.S. made the figures. A.D.S. and G.S.K.S. wrote the manuscript. All authors contributed to the manuscript and gave their final approval.

Notes

The authors declare no competing financial interest.

Raw data files are available at the Cambridge University Repository at <https://doi.org/10.17863/CAM.57720>.

ACKNOWLEDGMENTS

G.S.K.S. acknowledges funding from the Wellcome Trust (065807/Z/01/Z) (203249/Z/16/Z), the UK Medical Research Council (MRC) (MR/K02292X/1), Alzheimer Research UK (ARUK) (ARUK-PG013-14), Michael J. Fox Foundation (16238) and Infinitus China Ltd. We would like to thank Dr. Penny Hamlyn and Dr. Nadezhda Nespovitya for helpful discussions on chromatography protocols. We also thank Lyn Carter and Filomena Gallo of the Cambridge Advanced Imaging Centre for help with sample loading into the TEM. We thank Dr. Dijana Matak-Vinkovic for LC/MS sample analysis at the Department of Chemistry, University of Cambridge. We thank Maria Zachoropoulou for critical analysis of the manuscript.

REFERENCES

- (1) Jia, L., Zhao, W., Wei, W., Guo, X., Wang, W., Wang, Y., Sang, J., Lu, F., and Liu, F. (2020) Expression and Purification of Amyloid β -Protein, Tau, and α -Synuclein in *Escherichia Coli*: A Review. *Crit. Rev. Biotechnol.* 40, 475.
- (2) Soto, C., Castaño, E. M., Asok Kumar, R., Beavis, R. C., and Frangione, B. (1995) Fibrillogenesis of Synthetic Amyloid- β Peptides Is Dependent on Their Initial Secondary Structure. *Neurosci. Lett.* 200 (2), 105–108.
- (3) Pachahara, S. K., Chaudhary, N., Subbalakshmi, C., and Nagaraj, R. (2012) Hexafluoroisopropanol Induces Self-Assembly of β -Amyloid Peptides into Highly Ordered Nanostructures. *J. Pept. Sci.* 18 (4), 233–241.
- (4) Ryan, T. M., Caine, J., Mertens, H. D. T., Kirby, N., Nigro, J., Breheney, K., Waddington, L. J., Streltsov, V. A., Curtain, C., Masters, C. L., and Roberts, B. R. (2013) Ammonium Hydroxide Treatment of A β Produces an Aggregate Free Solution Suitable for Biophysical and Cell Culture Characterization. *PeerJ* 1, e73.

- (5) Finder, V. H., Vodopivec, I., Nitsch, R. M., and Glockshuber, R. (2010) The Recombinant Amyloid- β Peptide A β 1–42 Aggregates Faster and Is More Neurotoxic than Synthetic A β 1–42. *J. Mol. Biol.* 396 (1), 9–18.

- (6) Zagorski, M. G., Yang, J., Shao, H., Ma, K., Zeng, H., and Hong, A. (1999) Methodological and Chemical Factors Affecting Amyloid β Peptide Amyloidogenicity. *Methods Enzymol.* 309, 189–204.

- (7) Jia, L., Wang, W., Sang, J., Wei, W., Zhao, W., Lu, F., and Liu, F. (2019) Amyloidogenicity and Cytotoxicity of a Recombinant C-Terminal His 6 -Tagged A β 1–42. *ACS Chem. Neurosci.* 10 (3), 1251–1262.

- (8) Walsh, D. M., Thulin, E., Minogue, A. M., Gustavsson, N., Pang, E., Teplow, D. B., and Linse, S. (2009) A Facile Method for Expression and Purification of the Alzheimer's Disease-Associated Amyloid β -Peptide. *FEBS J.* 276 (5), 1266–1281.

- (9) Stephens, A. D., Nespovitya, N., Zacharopoulou, M., Kaminski, C. F., Phillips, J. J., and Kaminski Schierle, G. S. (2018) Different Structural Conformers of Monomeric α -Synuclein Identified after Lyophilizing and Freezing. *Anal. Chem.* 90 (11), 6975–6983.

- (10) Naslund, J., Schierhorn, A., Hellman, U., Lannfelt, L., Roses, A. D., Tjernberg, L. O., Silberring, J., Gandy, S. E., Winblad, B., and Greengard, P. (1994) Relative Abundance of Alzheimer A β Amyloid Peptide Variants in Alzheimer Disease and Normal Aging. *Proc. Natl. Acad. Sci. U. S. A.* 91 (18), 8378–8382.

- (11) Ramón, A., Señorale-Pose, M., and Marín, M. (2014) Inclusion Bodies: Not That Bad... *Front. Microbiol.* 5, 56.

- (12) Sun, S., Zhou, J. Y., Yang, W., and Zhang, H. (2014) Inhibition of Protein Carbamylation in Urea Solution Using Ammonium-Containing Buffers. *Anal. Biochem.* 446 (1), 76–81.

- (13) Krishtal, J., Bragina, O., Metsla, K., Palumaa, P., and Tõugu, V. (2015) Toxicity of Amyloid Beta 1–40 and 1–42 on SH-SY5Y Cell Line. *SpringerPlus* 4 (S1), 1–32.

- (14) Biancalana, M., and Koide, S. (2010) Molecular Mechanism of Thioflavin-T Binding to Amyloid Fibrils. *Biochim. Biophys. Acta, Proteins Proteomics* 1804, 1405–1412.

- (15) Klement, K., Wieligmann, K., Meinhardt, J., Hortschansky, P., Richter, W., and Fändrich, M. (2007) Effect of Different Salt Ions on the Propensity of Aggregation and on the Structure of Alzheimer's A β (1–40) Amyloid Fibrils. *J. Mol. Biol.* 373 (5), 1321–1333.

- (16) Arosio, P., Knowles, T. P. J., and Linse, S. (2015) On the Lag Phase in Amyloid Fibril Formation. *Phys. Chem. Chem. Phys.* 17 (12), 7606–7618.

- (17) Meisl, G., Yang, X., Hellstrand, E., Frohm, B., Kirkegaard, J. B., Cohen, S. I. A., Dobson, C. M., Linse, S., and Knowles, T. P. J. (2014) Differences in Nucleation Behavior Underlie the Contrasting Aggregation Kinetics of the A β 40 and A β 42 Peptides. *Proc. Natl. Acad. Sci. U. S. A.* 111 (26), 9384–9389.

- (18) Nag, S., Sarkar, B., Bandyopadhyay, A., Sahoo, B., Sreenivasan, V. K. A., Kombrabail, M., Muralidharan, C., and Maiti, S. (2011) Nature of the Amyloid- β Monomer and the Monomer-Oligomer Equilibrium. *J. Biol. Chem.* 286 (16), 13827–13833.

- (19) Banerjee, S., Hashemi, M., Lv, Z., Maity, S., Rochet, J. C., and Lyubchenko, Y. L. (2017) A Novel Pathway for Amyloids Self-Assembly in Aggregates at Nanomolar Concentration Mediated by the Interaction with Surfaces. *Sci. Rep.* 7 (1), 1–11.

- (20) Nilsberth, C., Westlind-Danielsson, A., Eckman, C. B., Condron, M. M., Axelman, K., Forsell, C., Stenh, C., Luthman, J., Teplow, D. B., Younkin, S. G., Näslund, J., and Lannfelt, L. (2001) The "Arctic" APP Mutation (E693G) Causes Alzheimer's Disease by Enhanced A β Protofibril Formation. *Nat. Neurosci.* 4 (9), 887–893.

- (21) Lu, M., Williamson, N., Mishra, A., Michel, C. H., Kaminski, C. F., Tunnacliffe, A., and Kaminski Schierle, G. S. (2019) Structural Progression of Amyloid- Arctic Mutant Aggregation in Cells Revealed by Multiparametric Imaging. *J. Biol. Chem.* 294 (5), 1478–1487.

- (22) Kummer, M. P., and Heneka, M. T. (2014) Truncated and Modified Amyloid-Beta Species. *Alzheimer's Res. Ther.* 6 (3), 28.

- (23) Schindelin, J., Arganda-Carreras, I., Frise, E., Kaynig, V., Longair, M., Pietzsch, T., Preibisch, S., Rueden, C., Saalfeld, S., Schmid, B., Tinevez, J. Y., White, D. J., Hartenstein, V., Eliceiri, K.,

Tomancak, P., and Cardona, A. (2012) Fiji: An Open-Source Platform for Biological-Image Analysis. *Nat. Methods* 9, 676–682.

(24) Young, L. J., Ströhl, F., and Kaminski, C. F. (2016) A Guide to Structured Illumination TIRF Microscopy at High Speed with Multiple Colors. *J. Visualized Exp.* No. 111, 53988.

(25) Müller, M., Mönkemöller, V., Hennig, S., Hübner, W., and Huser, T. (2016) Open-Source Image Reconstruction of Super-Resolution Structured Illumination Microscopy Data in ImageJ. *Nat. Commun.* 7 (1), 1–6.